manuscript KSJ

by Chua Pin Fen .

Submission date: 21-Nov-2024 03:13PM (UTC+0800)
Submission ID: 2527192611
File name: 1661_Chua_Pin_Fen_._manuscript_KSJ_6217_1686692237.docx (2.16M)
Word count: 6287
Character count: 36587

Title Page

Title: Advancing Parkinson's Disease Biopathology and Drug Discovery by Dual Cellular Modeling

Abbreviations:

6-OHDA

α-MG

α-syn

α-synucleinopathy

β-MG

DA

NS-1

PD

Abstract

Parkinson's disease (PD) is the fastest growing neurological disorder in the world. Its pathologic hallmarks are dopaminergic neuronal loss in the substantia nigra and alpha-synuclein accumulation in neurons. However, the patho-biologic mechanisms are largely unknown. Current drugs cannot slow or halt disease progression while clinical trials are mostly unsuccessful. Hence better cellular models are needed for pathological and drug discovery studies prior to *in vivo* validation. PC12 cells are commonly used for neurotoxicity studies but the Neuroscreen-1 (NS-1) variant has a faster doubling time and higher basal rate of neurite growth. We developed a NS-1 PD model with the neurotoxin 6-hydroxydopamine (6-OHDA) and MTT cell viability assay as readout. We optimized 6-OHDA concentration to a uniquely low 10 μM for a closer approximation to *in vivo* neurotoxicity. NS-1 cells treated with 6-OHDA displayed hallmark dopamine loss and apoptotic cell death. We used the model to screen a series of xanthones - polyphenolic compounds found in many medicinal plants. We report a novel activity of thwaitesixanthone in the PD model. The model was validated using alpha-mangostin (a neuroprotectant in *in vivo* and *in vitro* PD models) which was the most active in restoring cell viability. Alpha-synuclein is now a therapeutic target for stopping PD progression. Human HEK293 cells have neuronal attributes and reported to express pathologic alpha-synuclein. We hypothesized the transfection-efficient HEK293T cells is an optimal cell line for monitoring human alpha-synuclein levels. We make the first report that 6-OHDA treatment increased pathologic alpha-synuclein expression in HEK293T cells. This alpha-synucleinopathy model was validated using alpha-mangostin which attenuated 6-OHDA-induced pathologic alpha-synuclein to baseline levels. Thus we developed a novel NS-1 PD model more representative of *in vivo* neurotoxicity complemented by a human HEK293T cell-based alpha-synucleinopathy model for tracking pathologic alpha-synuclein levels. We present these dual models for producing *in vitro* findings with increased likelihood of clinical translation.

Keywords: 6-hydroxydopamine, PC12, NS-1, cellular model, alpha-synuclein, xanthone.

1. Introduction

Parkinson's disease (PD) is the fastest-growing neurological disorder in the world. Current PD drugs only treat the symptoms, without slowing down or stopping the underlying neurodegenerative processes (Stoker & Barker, 2020). The main pathological hallmark of PD is the loss of dopaminergic neurons in the substantia nigra pars compacta of the midbrain (Dauer & Przedborski, 2003). PD is also referred to as an α-synucleinopathy- a neurodegenerative disorder characterized by aggregated alpha-synuclein (α-syn) in neurons forming inclusions termed Lewy bodies (Koga et al., 2021). Currently α-syn is a therapeutic target and potential biomarker (Visanji et al., 2021). The classical PD motor symptoms such as resting tremor, bradykinesia and rigidity can be preceded by non-motor signs which have been attributed to synucleinopathy outside of the nigro-striatal pathway (Adler & Beach, 2016). Such dysfunction of other brain areas without a dopaminergic basis points to PD as a complex multisystem disorder.

Although postmortem brain analysis can shed light on end-stage PD, it is not possible to access the human brain or neurons to study the early stages. Hence it is necessary to develop experimental PD models that possess features of the dopaminergic system and reflect the disease phenotype (Lopes et al., 2017). The first PD animal model used rats injected with the neurotoxin 6-hydroxydopamine (6-OHDA), a hydroxylated metabolite of dopamine (DA) (Ungerstedt, 1968). Still widely used today, it selectively destroys catecholaminergic nerves to produce the PD behavioral phenotype, without formation of intracellular α-synuclein aggregates (Vareslija et al., 2020).

As animal studies are expensive and time consuming, *in vitro* models allow a controlled environment for rapid, cost-effective drug discovery and disease mechanism studies for further validation in primary neurons and *in vivo* models. Since clinical trials in PD have had a relatively low rate of success (Mathur et al., 2015), there is a pressing need for better preclinical models. One of the most used and cited cell lines for neurodegenerative studies is PC12, derived from a catecholamine-secreting tumor (pheochromocytoma)

of the rat adrenal medulla (Greene & Tischler, 1976). PC12 cells synthesize, store, secrete and take up catecholamines. Compared to rat chromaffin cells, its secretory vesicles contain more dopamine than norepinephrine (Wagner et al., 1993). Neuroscreen-1 (NS-1) is a subclone of PC12 cells with more robust growth and lesser cell aggregation (Chaurasiya et al., 2017). We had demonstrated its advantage over parental PC12 in its high basal level of neurite-expressing cells (Chua & Lim, 2021). Wild-type NS-1 cells have also been found to express higher levels of certain neuronal markers in comparison with PC12 (Pokharel et al., 2018). Thus we aimed to develop a NS-1 cell-based PD model using 6-OHDA.

Lewy bodies are found in human postmortem PD brain but there is no approved treatment available. Hence there is a need for cellular α-syn models both for pathobiologic studies and identification of compounds that abrogate its toxicity. In Lewy bodies, the pathologic α-syn is phosphorylated at serine 129 (pSer129-α-syn) (Kim et al., 2019). Wild type human HEK293 cells have been reported to express endogenous pSer129-α-syn detectable by western blotting (Sasaki et al., 2015). As studies often require transfection of exogenous proteins, we aimed to develop a PD cellular model using the highly transfection-efficient HEK293T cells for studying 6-OHDA-induced pathologic α-syn levels. This α-syn model will complement the NS-1 neurotoxicity cell death model to provide dual *in vitro* modeling of PD for better clinical translation

2. Materials and Methods

2.1 Reagents and chemicals

Culture medium DMEM high glucose, horse serum, fetal bovine serum and N2 supplement were from Gibco (Grand Island, NY). Collagen IV were from Advanced Biomatrix (Carlsbad, CA). Alpha-mangostin and beta-mangostin were from MedChemExpress (Monmouth, NJ). 3-(4,5-dimethylthiazol-2-yl)-2,5-

diphenyltetrazolium bromide) tetrazolium salt, 6-hydroxydopamine hydrobromide (6-OHDA) and N-Acetyl-Asp-Glu-Val-Asp-al (caspase inhibitor) and all other biochemical reagents were from Sigma-Aldrich (St. Louis, MO).

2.2 Preparation of trapezifolixanthone, brasixanthone B, ananixanthone and thwaitesixanthone

Powdered air-dried stem barks of *Calophyllum spp* were extracted with solvents (5 L) (n-hexane, chloroform, ethyl acetate and methanol) by cold maceration for 72 hours at room temperature in a closed vessel. The extracts were filtered using filter paper and concentrated under reduced pressure in a rotary evaporator to yield the crude extracts.

The isolation work on stem bark extracts of *Calophyllum spp* was performed using column chromatography techniques. Structural elucidation was by spectroscopic methods including 1D NMR, 2D NMR and MS. The extracts were subjected to VLC using Silica gel 60 PF254 1.07749 Merck using gradient elution method with the solvent system [*n*-hexane-chloroform, chloroform- ethyl acetate, ethyl acetate-methanol with increasing polarity (Hex: $CHCl_3$: 100: 0) to (EA: MeOH: 5:5)] as the mobile phase to give sub-fractions. Fractions that show a similar pattern on TLC were pooled and subjected to column chromatography. A series of column chromatography separations using silica gel 60 (Merck 1.09385, 0.040–0.063 mm) were performed using the same mobile phase system as the solvent system. The fractions were further separated by gel filtration chromatography using Sephadex LH-20 and methanol as the eluent. The sub-fractions with similar pattern on TLC profile were combined and subjected to further purification using radial chromatography to isolate the pure compounds trapezifolixanthone, brasixanthone B, ananixanthone and thwaitesixanthone.

2.3 Preparation of 6-OHDA stock solution

6-OHDA-Hbr (1.47 mg) was dissolved in 1.33 mL of 0.15% chilled ascorbic acid to produce 3 mM of stock solution. The correction factor for 6-OHDA-Hbr is 1.47. The stock solution was stored at -80°C and diluted to the desired concentration with Hanks' Balanced Salt Solution (HBSS) before cell treatment.

2.4 Cell culture and treatment

Rat pheochromocytoma (PC12) cells Neuroscreen-1 (NS-1) variant, (formerly from Cellomics), were a kind gift from Dr. Yves Le Dréan, University of Rennes 1, France. NS-1 cells were cultured in DMEM supplemented with 2.5% fetal bovine serum and 15% horse serum in a collagen IV-coated tissue culture flask/well. The coating protocol followed the published method (Chua & Lim, 2023). Cell cultures were incubated in a chamber at 37 °C under 5% CO_2. Cells used for experiments were those that had been passaged between 3 and 13 times. HEK293T cells were a generous gift from Dr. Richard Neubig while at the University of Michigan, USA. HEK293T cells were cultured in DMEM supplemented with 10% fetal bovine serum in a polystyrene tissue culture flask. For determining the IC_{50} of 6-OHDA on NS-1 cells, cells were seeded into 96-well collagen IV-coated plates with a density of 4 x 10^3 cells / well. After 24 hours of incubation at 37 °C under 5% CO_2, cells were treated with DMEM-supplemented media alone or with 0 μM, 2.5 μM, 5 μM, 7.5 μM, 10 μM, 12.5 μM, 15 μM, 20 μM and 50μM 6-OHDA for 24 hours. After 24 hours, cell confluency and morphology were observed under an inverted microscope (Olympus IX 73) with image acquisition using Olympus cellSens Dimension 2.2 before the cell viability assay.

2.5 Dopamine secretion by enzyme-linked immunosorbent assay

The dopamine secretion of NS-1 cells was detected using a dopamine ELISA kit (ENZO, USA). Briefly, cells were seeded in a collagen IV-coated 96-well clear plate. After 24 hours, cells were treated with or without α-MG for 2 hours followed by 48 hours of 10 μM of 6-OHDA treatment. After 48 hours, cell media supernatant was collected after centrifuging at 1000 x g, 2-8° C, for 20 minutes. The ELISA

plate was washed once before adding the sample and standard. Fifty µL of each sample was added to the wells, followed by 50 μl biotin-detection antibody. The plate was incubated at 37 °C for 45 minutes. The solution was discarded, and the plate was washed three times. Horseradish peroxidase-streptavidin conjugate was added to the well and incubated at 37ºC for 30 minutes. After washing five times, 90 µL of TMB substrate was added into each well, and the sample was incubated at 37 ºC in the dark for 15-20 min. Fifty μL of stop solution was added to each well. The result was read at 450 nm using a microplate reader (SpectraMax iD3, Molecular Devices, Austria) (Tang et al., 2012).

2.6 Quantification of α-synuclein protein expression by western blotting

Treatment of HEK293T cells with α-MG was performed by a 2-hour incubation with α-MG followed by 24 hours of 6-OHDA treatment. HEK293T cells were lysed in lysis buffer (50 mM Tris-HCl, pH 8, 150 mm NaCl, 0.5% sodium deoxycholate, 0.1% SDS (sodium dodecyl sulfate), 1% Nonidet P40, 2 μg/mL aprotinin, 10 μg/mL leupeptin, 1 mM AEBSF and 4mM sodium orthovanadate then centrifuged at 16,000 g for 20 minutes at 4 ºC. Twenty μg of cell extract was separated on 15% SDS-PAGE gels and transferred to 0.45 μm PVDF membranes. Immediately after the transfer, the membrane was fixed with 4% paraformaldehyde and 0.1% glutaraldehyde for 30 mins, followed by western blotting. Western blotting was carried out using the Fast Western Blot Kit (Thermo Fisher Scientific) according to the manufacturer's instructions. Briefly, membranes were probed with 1:1000 alpha-synuclein (Syn211) mouse monoclonal primary antibody (Thermo Fisher Scientific)/alpha-synuclein (phosphorylated-alpha-synuclein (pSer129-α-syn) rabbit primary antibody (Abcam) for 30 min. GAPDH was used as a loading control for protein normalization. The blot was incubated with diluted Optimised HRP Reagent (Thermo Fisher Scientific) and visualised by chemiluminescence after incubation with SuperSignal West Dura Substrate® (Thermo Fisher Scientific). Images were captured and analyzed with the Amersham Imager 680 system (GE Healthcare Bio-Sciences Corp, Piscataway, US). The band intensity was quantified by the Amersham Imager 680 system.

2.7 Cell viability assay

Cell viability was measured using the MTT (3-(4,5-dimethylthiazol-2-yl)-2,5-diphenyltetrazolium bromide) tetrazolium assay. MTT assay was carried out by removing the supernatant to a medium containing 0.5 mg/mL MTT for three hours at 37 °C. The supernatant was removed and replaced with 100 μL DMSO. The plate contents are mixed on a rotary shaker at room temperature for 10 min. Subsequently, absorbance was read at 570 nm with an Infinite 200 Pro microplate reader (Tecan, Switzerland).

2.8 Treatment with drug/compounds

NS-1 cells were seeded at a density of 4 x 10^3 cells / well into collagen IV-coated 96-well clear plate. Cells were incubated for 24 hours at 37 °C under 5% CO_2, humidified incubator. Thirty μM caspase-3 inhibitor (Ac-DEVD-CHO) was used to treat the cells for 2 hours before 6-OHDA treatment. Then, the medium was changed to a fresh medium alone or a medium containing 10 μM 6-OHDA media with or without the caspase-3 inhibitor for 24 hours, followed by MTT assay to investigate the predominant cell death mechanism involving caspase.

For validation of the *in vitro* PD model, the same procedure was used with the compounds 1 nM alpha-mangostin, 1 nM β-MG, 10 nM brasixanthone B, 10 nM ananixanthone, 100 nM thwaitesixanthone or 100 nM trapezifolixanthone instead of caspase inhibitor. The concentrations used were not cytotoxic and represent the lowest concentration that gave the maximal effect. The same method was used for treatment of HEK293T cells for collection of cell lysate except the concentration of 6-OHDA was 25 μM and cells were grown in 6-well dishes for cell lysate collection.

2.9 Statistical analysis

All data were analyzed using Prism 9 software (GraphPad, La Jolla, CA). Data sets were tested for statistical significance using, one-way ANOVA followed by post hoc Tukey's test or Dunnett's test for comparing three or more data groups. Differences were considered statistically significant when $p < 0.05$. Experiments were repeated three times, with each performed in triplicate. Data were reported as mean ± SEM.

3. Result

3.1 6-OHDA induces concentration-dependant cell death in NS-1 cells with IC_{50} of ~10 µM

NS-1 cells were subjected to various concentrations of 6-OHDA, including a control group treated with media alone. Cells were treated for 24 hours then cell viability measured via MTT assay, as shown in Figure 1. Cell viability of NS-1 cells reduced in a dose-response manner with a IC_{50} of 10.52 µM.

At 10 µM 6-OHDA, cell viability decreased significantly to 55.6% ± 2.73% ($p < 0.05$, compared to the control group) and this concentration was selected for establishing a PD cellular model using NS-1 cells.

NS-1 cells underwent a 24-hour treatment with either media alone or 6-OHDA. Figure 2 shows representative microscopic images depicting the cellular response to 6-OHDA at 5 μM, 10 μM, and 20 μM. Figure 2A shows NS-1 cells without 6-OHDA treatment as baseline control. NS-1 cells treated with 5 μM 6-OHDA exhibited predominantly healthy morphological characteristics (see Figure 2B). In Figure 2C, NS-1 cells subjected to a 10 μM 6-OHDA displayed a heterogeneous cellular population, featuring both normal and rounded or shrunk cells. At 20 μM (Figure 2D) the majority of the cells were rounded and phase-bright (loss of cell-substratum adhesion).

3.2 6-OHDA induces NS-1 cell death through activation of the caspase pathway

Apoptosis is the main mechanism of neuronal death in PD (Erekat, 2018). We used Ac-DEVD-CHO, a caspase-3 inhibitor, to investigate the mechanism of 6-OHDA-induced NS-1 cell death. NS-1 cells were

subjected to a 24-hour incubation with 10 μM 6-OHDA, with or without treatment with 30 μM Ac-DEVD-CHO. Ac-DEVD-CHO was added to NS-1 cells two hours before the 6-OHDA treatment, followed by a 24-hour exposure to 10 μM of 6-OHDA. After exposure to 10 μM 6-OHDA (Figure 3), MTT assay showed a reduction in NS-1 cell viability of 54.8 ± 3.7% ($p < 0.01$). Ac-DEVD-CHO inhibited cell death and significantly restored cell viability in 6-OHDA-treated NS-1 cells to 89.7 ± 3.3% ($p < 0.05$), suggesting that the NS-1 cell death induced by 6-OHDA is predominantly via apoptosis.

3.3 NS-1 cell-based PD model mimics pathology of PD by reducing dopamine secretion following 6-OHDA treatment

The dopaminergic neurons of the nigro-striatal pathway synthesize and release the neurotransmitter DA. In NS-1 cells, DA is secreted into the cell supernatant as detected by an ELISA assay. PD motor symptoms arise from decrease in striatal DA (Sayyaed et al., 2023). A 48-hour treatment of NS-1 cells with 6-OHDA lowered dopamine secretion to 62.1 ± 6.6% of untreated cells (control) normalized to 100% (Figure 4). Alpha-mangostin is a polyphenolic xanthone reported to reverse the PD phenotype in a rat model (Parkhe et al., 2020). In 6-OHDA-treated cells, addition of 1 nM α-MG almost fully restored the loss of dopamine secretion by restoring it to 91.0 ± 5.0% ($p < 0.01$) of untreated NS-1 cells.

3.4 Treatment with 6-OHDA increases protein levels of pathologic alpha-synuclein (pSer129-α-syn) in HEK293T cells

In Lewy bodies, the pathologic α-syn is phosphorylated at serine 129 (pSer129-α-syn) (Kim et al., 2019). Endogenous pSer129-α-syn has been reported to be detectable by western blotting in wild type human HEK293 cells (Sasaki et al., 2015). To investigate HEK293T cells as an α-synucleinopathy model, western blotting for pSer129-α-syn in wild type HEK293T cell lysates (using the same protocol as for NS-1 cells) revealed a ~16kDa band corresponding to pSer129-α-syn. HEK293T cells had a higher resistance to 6-

OHDA toxicity compared to NS-1 cells. To optimize the concentration of 6-OHDA, HEK293T cells were treated with 10 μM, 25 μM and 50 μM 6-OHDA. Twenty-five μM was selected for optimal expression of α-syn (data not shown). Treatment with 25 μM 6-OHDA in HEK293T cells resulted in a substantial augmentation of pSer129-α-syn expression as shown in Figure 5B. We also investigated the expression of non-phosphorylated α-syn in HEK293T cells using the Syn211 α-syn antibody for human targets. Figure 5A shows the endogenous wild type α-syn in HEK293T cells but unlike pathologic α-syn its expression level was essentially unchanged after 6-OHDA treatment.

Figure 5C shows the quantification of pSer129-α-syn expression, normalized against GADPH. Treatment with 6-OHDA raised pSer129-α-syn expression ~1.7-fold in HEK293T cells ($p < 0.05$). Pretreatment with 1 μM α-MG for 2 hours, followed by a 24-hour exposure to 6-OHDA, significantly attenuated pSer129-α-syn expression to baseline level ($p < 0.01$).

3.5 NS-1 cell-based PD model is an effective screen for potential antiparkinsonian drugs

We validated our experimental model for drug screening with six xanthones: α-MG, β-MG, ananixanthone, trapezifolixanthone, thwaitesixanthone, and brasixanthone B. Alpha-mangostin has been found effective in PD models while β-MG has not been reported for neuroprotective activity (Le et al., 2023). We previously reported ananixanthone but not trapezifolixanthone to be active in a stroke model, but much less is known about thwaitesixanthone or brasixanthone B.

We screened the xanthones for activity to restore cell viability after 6-OHDA treatment. As a control, the compounds tested did not have a direct proliferative effect on untreated NS-1 cells (Figure 6A). To assess their ability to restore cell viability in 6-OHDA-treated NS-1 cells, we added the xanthones to the cells 2 hours before adding 6-OHDA for a 24-hour incubation. The xanthones were screened at four concentrations (1 nM, 10 nM, 100 nM, and 1 μM, data not shown) and the lowest concentration giving maximal response is shown in Figure 6B.

After 6-OHDA treatment, cell viability was reduced to 58.8 ± 2.2%. Among the six xanthones tested, 1 nM α-MG restored cell viability to the highest level of 87.8 ± 8.7% ($p < 0.0001$). Four xanthones- 100 nM thwaitesixanthone, 10 nM ananixanthone, 10 nM β-MG, and 1 nM brasixanthone B increased cell viability significantly to 86.5 ± 4.2% ($p < 0.0001$), 79.3 ± 3.9% ($p < 0.001$), 78.7 ± 4.4% ($p < 0.01$), and 78.2 ± 7.9% ($p < 0.01$), respectively. Trapezifolixanthone (100 nM) restored cell viability to 72.1 ± 6.4%.

4. Discussion

Despite the number of antiparkinsonian drugs in use, none can modify the underlying neurodegenerative processes. Almost all current approved PD drugs act on a single molecular target (Cheong et al., 2019). As PD is a multifactorial, multisystem disease, single-target drugs are more likely to only provide symptomatic relief. The identification of disease-modifying drugs is more probable with phenotypic screening for compounds that can reverse the disease phenotype rather than (single) target-based screening (Cetin et al., 2022). Cellular models are rapid, inexpensive and do not need ethical approval. They can accommodate high-content screening (via imaging) as well as accommodate genetic or pharmacological manipulations (Falkenburger et al., 2016). They also facilitate the study of disease mechanisms through simplifying complex networks and pathological processes into simpler molecular events. We report here the first cellular PD model based on NS-1 cells for biopathologic studies and phenotypic screening of potential drugs.

As clinical trials for PD are frequently unsuccessful, it is critical to have cellular disease models that reflect PD pathobiology and the neuronal character of the diseased cells. PC12 cells express DA receptors (Zhang et al., 2019) together with the cellular machinary for the synthesis and secretion of DA. They also express the DA transporter (DAT) for the uptake of 6-OHDA (Wiesinger et al., 2007). Morphologically, wild type NS-1 cells have a higher basal level of neurite outgrowth compared to parental PC12 cells (Chua & Lim,

2021). They also express higher levels of certain neuronal markers compared to PC12 cells (Pokharel et al., 2018). The main pathological hallmark of PD is the loss of dopaminergic neurons in the substantia nigra pars compacta (mainly by apoptosis) (Erekat, 2022) with depletion of DA levels in the striatum (Dauer & Przedborski, 2003). We showed in the NS-1 cellular PD model that 6-OHDA neurotoxin treatment reduced dopamine secretion by ~40% while ~90% of the cells died by apoptosis. We validated this model for drug screening by the ability of the established PD neuroprotectant α-MG to reverse both the 6-OHDA-induced apoptosis and DA lowering in NS-1 cells.

Our NS-1 PD model based on 6-OHDA has one critical difference from published PC12 cell models. Mejia and colleagues reported the range of neurotoxic 6-OHDA concentrations used in PC12 viability assays were from 20 μM to 1000 μM (Mejía et al., 2013), which is relatively high. In contrast, we optimized 6-OHDA concentration in the NS-1 PD model to a significantly low 10μM. High 6-OHDA concentrations may compromise the PD model in several ways. While neuronal loss in PD is mainly by apoptosis, 6-OHDA can produce neuronal death via other mechanisms including necrosis, autophagy and catastrophic cell rupture (Vareslija et al., 2020). A lower concentration of 6-OHDA more closely resembles PD pathology as it has been reported that 25 μM 6-OHDA in PC12 cells resulted in apoptosis, but 50 μM produced a mixture of apoptosis and necrosis (Ochu et al., 1998). In rat neuronal cultures, 6-OHDA concentrations higher than 10 μM acted like a non-selective toxin that destroyed both dopaminergic and non-dopaminergic cells, likely via extracellular processes such as 6-OHDA-induced auto-oxidation and induction of oxidative stress from the oxidative products generated (Hanrott et al., 2006). It was concluded that low 6-OHDA concentrations were selectively toxic for dopaminergic neurons and utilized the dopamine transporter for 6-OHDA uptake into neuronal terminals (Vareslija et al., 2020). Hence our NS-1 PD model based on 10 μM 6-OHDA avoids generating excessive non-selective toxicity to better mimic *in vivo* neurotoxin-induced PD with the objective that findings can have a greater likelihood of translation into *in vivo* settings, and ultimately in humans. Furthermore, our optimized PD model produces 40-50% mortality in NS-1 cells with

318 approximately equal numbers of healthy and rounded cells. As Ryou and Mallet had cautioned, a high
319 mortality rate may preclude any rescue intervention under study (Ryou & Mallet, 2018). We also optimized
320 cell seeding to obtain a cell confluency of 40-60% because high cellular confluency can render a protective,
321 anti-cytotoxic effect (Ryou & Mallet, 2018) necessitating the use of higher 6-OHDA concentrations.

322

323 Lewy bodies are found in human postmortem PD brain but there is no approved treatment available. The
324 6-OHDA animal PD model does not produce Lewy bodies (Schober, 2004). In rat models, the 6-OHDA
325 neurotoxin and α-syn PD models replicate different aspects of pathophysiology resulting in different
326 neuropathological characteristics (Decressac et al., 2012). Hence there is a need for cellular α-syn models
327 both for pathobiologic studies and identification of compounds to abrogate its toxicity. Sasaki and
328 colleagues detected both α-syn and pSer129-α-syn in untransfected, untreated HEK293 cells (Sasaki et
329 al., 2015). Thus far there is no published study on α-syn expression following 6-OHDA treatment in
330 HEK293-derived cells. We found 6-OHDA increased expression of endogenous pathologic pSer129-α-
331 syn but not non-pathological unphosphorylated α-syn and provide the first report that 6-OHDA induces
332 pathologic α-syn expression in HEK193T cells. We validated this model for drug screening by
333 demonstrating that the known PD neuroprotectant, α-MG, attenuated the expression of the 6-OHDA-
334 induced pathologic pSer129-α-syn to baseline level. Thus we established an α-synucleinopathy model
335 based on wild type HEK293-derived cells.

336

337 For better clinical translation, this HEK293T α-synucleinopathy model tracks endogenously-expressed α-
338 syn rather than exogenously-sourced and externally added (or transfected) α-syn or its preformed fibrils.
339 The use of HEK293T cells is advantageous as it supports high transfection efficiency (Lin et al., 2014)
340 should any exogenous protein overexpression be needed to investigate signaling mechanisms. Although
341 HEK293 is not a neuronal cell line, it has neuronal proteins and attributes showing it likely originated

342 from a cell type with neuronal lineage (Shaw et al., 2002). Despite its origin from human kidney, it is
343 relevant as an α-synucleinopathy model because α-syn is highly expressed in non-neuronal tissues
344 including blood, kidney and adipose tissues (Hallacli et al., 2022) while its overall precise role in PD
345 pathogenesis is still not well understood. As an example, it has been proposed that Lewy type α-
346 synucleinopathy in organs outside of the brain may play a role in non-motor PD symptoms (Adler &
347 Beach, 2016). Since α-syn aggregates can spread throughout the central nervous system, α-syn is
348 considered a therapeutic target for stopping PD progression. Hence we present a HEK293T cell-based α-
349 synucleinopathy model for investigating pathologic α-syn accumulation and drugs that reverse it.

350

351 Xanthones have bioactivity in numerous disease models and is increasingly used in drug development
352 (Ruan et al., 2017). We had previously shown ananixanthone to be active in a stroke model, with lesser
353 activity by trapezifolixanthone (Lizazman et al., 2022). We used α-MG as a positive control because it
354 was found effective in a neuroblastoma-cell (Hao et al., 2017), rat (Parkhe et al., 2020) and mouse
355 (Parekh et al., 2022) PD models. In contrast, aside from inhibition of acetylcholinesterase (Le et al.,
356 2023), β-MG has not been studied in other neurological disease models. Much less has been reported for
357 thwaitesixanthone and brasixanthone B. Our data corroborates α-MG's reported antiparkinsonian activity
358 and its abrogation of pathologic α-syn expression in PD models. Beta-mangostin and trapezifolixanthone
359 were comparatively less active in our NS-1 PD model. We screened 6 xanthones with our model and
360 report a novel activity of thwaitesixanthone that is comparable to α-MG.

361 **5. Conclusion**

362

363 Disease-modifying drugs are being sought for PD but clinical trials frequently fail. This can be due to
364 findings from *in vitro* models being unable to be translated into *in vivo* settings. This study presents the
365 dual development of the NS-1 cellular PD and HEK293T α-synucleinopathy models to address this

problem. Compared to parental PC12 cells, NS-1 cells grow more rapidly and possess greater neuronal attributes. We used a uniquely low 6-OHDA neurotoxin concentration to more closely mimic neurotoxcity in animals. As proof of concept for a PD drug screening model, we studied a series of xanthones and provide the first report that thwaitesixanthone is neuroprotective in a cellular PD model. We also provide the first demonstration that 6-OHDA induces pathologic α-syn expression in HEK293T cells and thus establish a cellular α-synucleinopathy model. We validated this model using α-MG, a known neuroprotectant, to attenuate the pathologic α-syn expression. We present these dual models for advancing biopathological understanding of PD and accelerating successful PD drug discovery.

Acknowlegements:

We thank Universiti Malaysia Sarawak for administrative support of the project and Sarawak Research and Development Council Sarawak, Malaysia for funding the project.

Funding:

This work was funded by a Catalyst Grant (GL/F05/SRDC/10/2020) from Sarawak Research and Development Council, Sarawak, Malaysia.

Conflicts of interest: The authors declare no conflict of interest

388 **Figure legends**

389 Figure 1: Determination of half maximal inhibitory concentration of 6-OHDA for NS-1 cells. The results
390 are expressed as mean +/- SEM of 3 independent experiments.

391 Figure 2: Cellular morphology of NS-1 cells after a range of concentrations of 6-OHDA treatment. (A)
392 untreated NS-1 cell (control), 0 μM (B) 5 μM (C) 10 μM (D) 20 μM. Scale bar 100 μm.

393 Figure 3: Cell viability of NS-1 cells and 6-OHDA-treated NS-1 cells with or without Ac-DEVD-CHO
394 treatment. Cell viability is normalized to untreated NS-1 cells (control). All data are expressed as
395 mean ± SEM of 3 experiments determined in triplicate. *$p < 0.05$, **$p < 0.01$

396 Figure 4: DA secretion of NS-1 cells and 6-OHDA-treated NS-1 cells with or without α-MG treatment. DA
397 level is normalized to untreated NS-1 cells (control). All data are expressed as mean ± SEM of 3 to 5
398 experiments determined in triplicate. **$p < 0.01$, ****$p < 0.0001$

399 Figure 5: Western blot analysis of α-syn and pSer129-α-syn protein expression in HEK293T cells. (A) α-
400 syn expression in HEK293T cells shows no difference between untreated cells (lane 1) and those treated
401 with 6-OHDA (lane 2). (B) pSer129-α-syn expression in HEK293T cells is increased after treatment with
402 6-OHDA (lane 2) compared to untreated HEK293T cells (lane 1). Expression of pSer129-α-syn in 6-
403 OHDA-treated HEK293T cells is reduced after treatment with α-MG (lane 3) compared to 6-OHDA-treated
404 only (lane 2). Data shown is from 1 experiment representative of at least 3 experiments. (C) Densitometric
405 analysis of pSer129-α-syn band relative to GADPH in HEK293T cells. Data is expressed as mean ± SEM
406 of 3 experiments. *$p < 0.05$, **$p < 0.01$.

407 Figure 6: (A) Cell viability of compound-treated cells without 6-OHDA treatment. NS-1 cells were treated
408 with the indicated compounds as described under "Treatment with compounds". Cell viability was
409 measured with MTT assay. (B) Application of NS-1 cell-based PD model in compound screening using
410 cell viability assay on 6-OHDA-treated cells. Cells were incubated with α-MG, β-MG, ananixanthone,
411 brasixanthone B, thwaitesixanthone and trapezifolixanthone for 2 hours followed by 24 hours of incubation

with 10 μM 6-OHDA. Data was normalized to control. All data are expressed as mean ± SEM of 3-5 experiments determined in triplicate. *p < 0.05, **p < 0.01, ***p< 0.001, ****p< 0.0001.

Figures

Fig 1

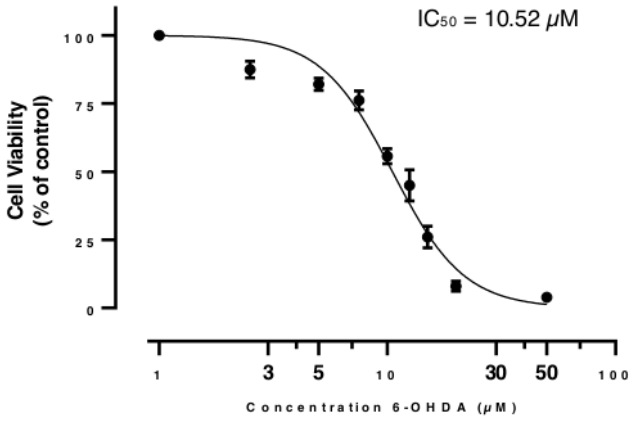

Fig 2

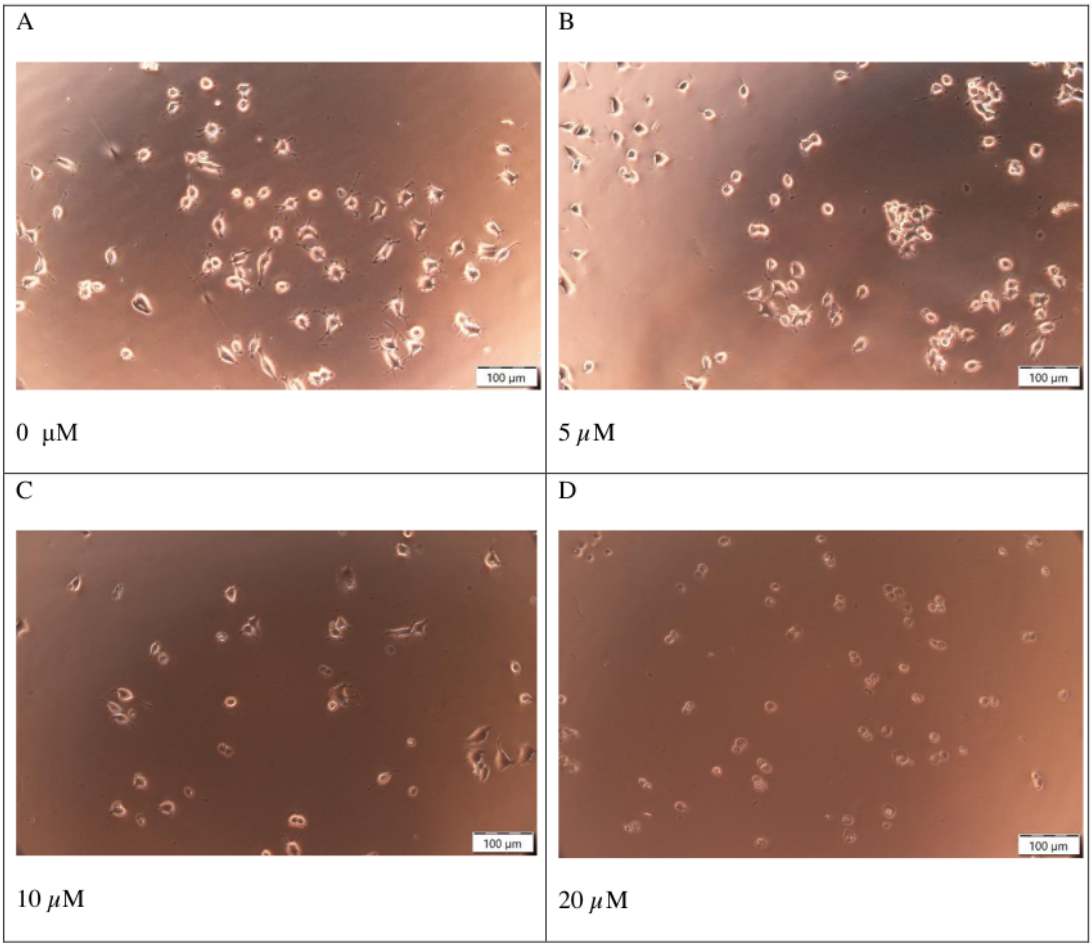

Fig 3

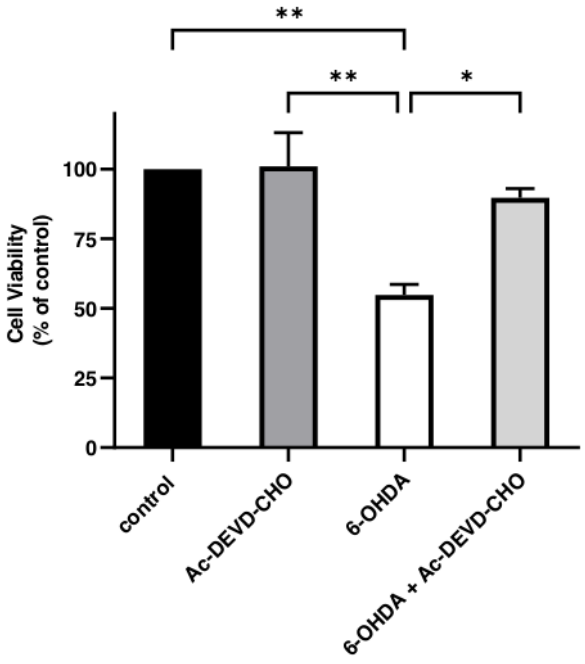
**
**
*
Cell Viability
(% of control)
100
75
50
25
0
control
Ac-DEVD-CHO
6-OHDA
6-OHDA + Ac-DEVD-CHO

Fig 4

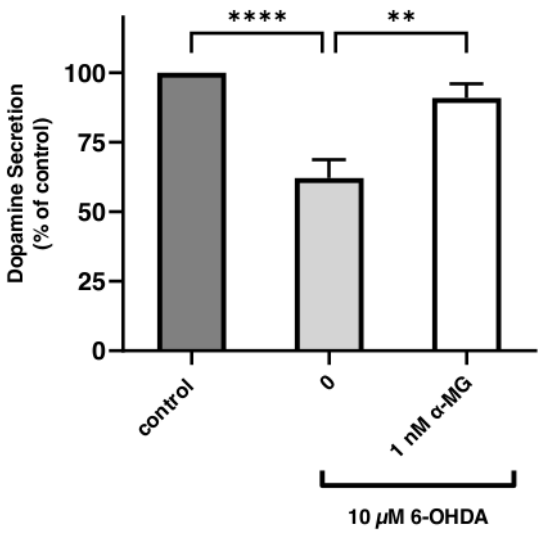
****
**
Dopamine Secretion
(% of control)
100
75
50
25
0
control
0
1 nM α-MG
10 μM 6-OHDA

Fig 5

A

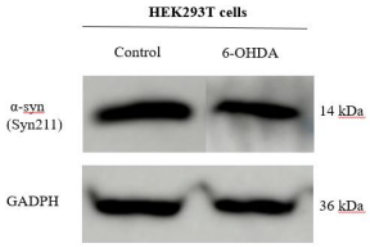
HEK293T cells
Control
6-OHDA
α-syn
(Syn211)
14 kDa
GADPH
36 kDa

B

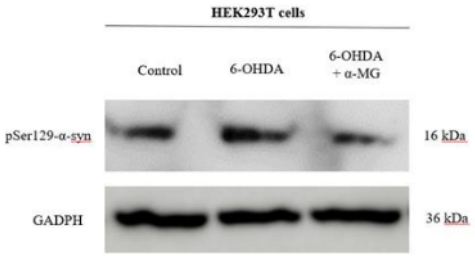
HEK293T cells
Control
6-OHDA
6-OHDA
+ α-MG
pSer129-α-syn
16 kDa
GADPH
36 kDa

C

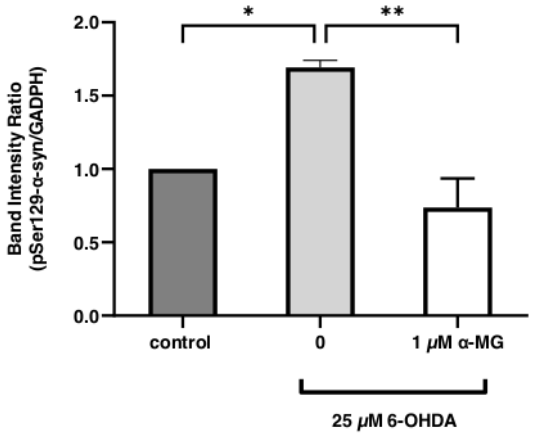
Band Intensity Ratio
(pSer129-α-syn/GADPH)
2.0
1.5
1.0
0.5
0.0
*
**
control
0
1 μM α-MG
25 μM 6-OHDA

Fig 6

A

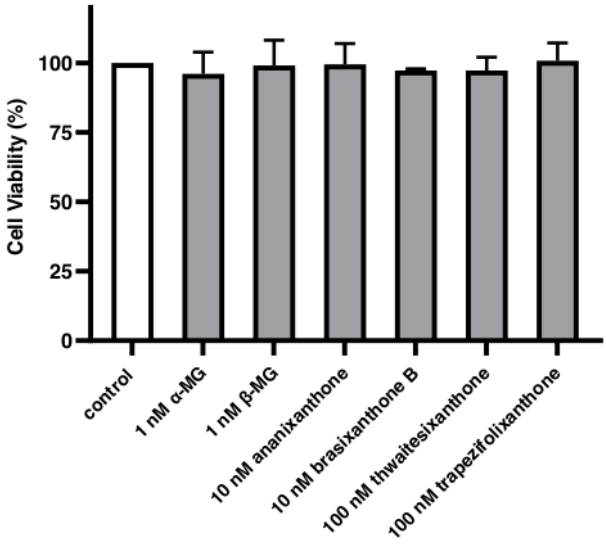
Cell Viability (%)
100
75
50
25
0
control
1 nM α-MG
1 nM β-MG
10 nM ananixanthone
10 nM brasixanthone B
100 nM thwaitesixanthone
100 nM trapezifolixanthone

B

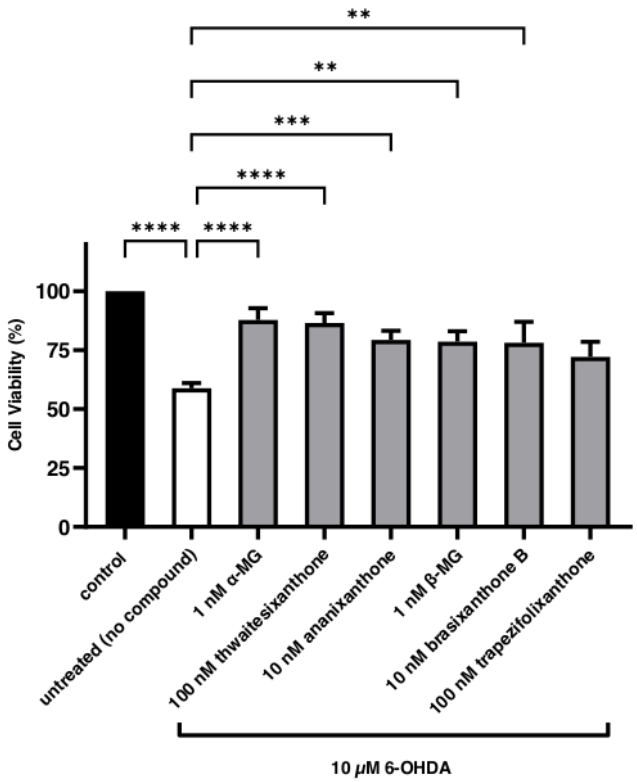

References

Adler, C. H., & Beach, T. G. (2016). Neuropathological basis of nonmotor manifestations of Parkinson's disease. *Mov Disord*, *31*(8), 1114-1119. https://doi.org/10.1002/mds.26605

Cetin, S., Knez, D., Gobec, S., Kos, J., & Pislar, A. (2022). Cell models for Alzheimer's and Parkinson's disease: At the interface of biology and drug discovery. *Biomed Pharmacother*, *149*, 112924. https://doi.org/10.1016/j.biopha.2022.112924

Chaurasiya, N. D., Shukla, S., & Tekwani, B. L. (2017). A Combined In Vitro Assay for Evaluation of Neurotrophic Activity and Cytotoxicity. *SLAS Discov*, *22*(6), 667-675. https://doi.org/10.1177/2472555217698677

Cheong, S. L., Federico, S., Spalluto, G., Klotz, K. N., & Pastorin, G. (2019). The current status of pharmacotherapy for the treatment of Parkinson's disease: transition from single-target to multitarget therapy. *Drug Discov Today*, *24*(9), 1769-1783. https://doi.org/10.1016/j.drudis.2019.05.003

Chua, P., & Lim, W. K. (2021). Optimisation of a PC12 cell-based in vitro stroke model for screening neuroprotective agents. *Scientific reports*, *11*(1), 8096-8096. https://doi.org/10.1038/s41598-021-87431-4

Chua, P., & Lim, W. K. (2023). The strategic uses of collagen in adherent cell cultures. *Cell Biol Int*, *47*(2), 367-373. https://doi.org/10.1002/cbin.11966

503 Dauer, W., & Przedborski, S. (2003). Parkinson's disease: mechanisms and models. *Neuron*, *39*(6), 889-
504 909. https://doi.org/10.1016/s0896-6273(03)00568-3
505 Decressac, M., Mattsson, B., & Bjorklund, A. (2012). Comparison of the behavioural and histological
506 characteristics of the 6-OHDA and alpha-synuclein rat models of Parkinson's disease. *Exp Neurol*,
507 *235*(1), 306-315. https://doi.org/10.1016/j.expneurol.2012.02.012
508 Erekat, N. S. (2018). Apoptosis and its Role in Parkinson's Disease. *Exon Publications*, 65-82.
509 Erekat, N. S. (2022). Apoptosis and its therapeutic implications in neurodegenerative diseases. *Clinical*
510 *Anatomy*, *35*(1), 65-78.
511 Falkenburger, B. H., Saridaki, T., & Dinter, E. (2016). Cellular models for Parkinson's disease. *J*
512 *Neurochem*, *139 Suppl 1*, 121-130. https://doi.org/10.1111/jnc.13618
513 Greene, L. A., & Tischler, A. S. (1976). Establishment of a noradrenergic clonal line of rat adrenal
514 pheochromocytoma cells which respond to nerve growth factor. *Proc Natl Acad Sci U S A*, *73*(7),
515 2424-2428. https://doi.org/10.1073/pnas.73.7.2424
516 Hallacli, E., Kayatekin, C., Nazeen, S., Wang, X. H., Sheinkopf, Z., Sathyakumar, S., Sarkar, S., Jiang, X.,
517 Dong, X., Di Maio, R., Wang, W., Keeney, M. T., Felsky, D., Sandoe, J., Vahdatshoar, A., Udeshi, N.
518 D., Mani, D. R., Carr, S. A., Lindquist, S., . . . Khurana, V. (2022). The Parkinson's disease protein
519 alpha-synuclein is a modulator of processing bodies and mRNA stability. *Cell*, *185*(12), 2035-
520 2056 e2033. https://doi.org/10.1016/j.cell.2022.05.008
521 Hanrott, K., Gudmunsen, L., O'Neill, M. J., & Wonnacott, S. (2006). 6-hydroxydopamine-induced
522 apoptosis is mediated via extracellular auto-oxidation and caspase 3-dependent activation of
523 protein kinase Cδ. *Journal of biological chemistry*, *281*(9), 5373-5382.
524 https://doi.org/10.1074/jbc.M511560200
525 Hao, X. M., Li, L. D., Duan, C. L., & Li, Y. J. (2017). Neuroprotective effect of alpha-mangostin on
526 mitochondrial dysfunction and alpha-synuclein aggregation in rotenone-induced model of
527 Parkinson's disease in differentiated SH-SY5Y cells. *J Asian Nat Prod Res*, *19*(8), 833-845.
528 https://doi.org/10.1080/10286020.2017.1339349
529 Kim, S., Kwon, S. H., Kam, T. I., Panicker, N., Karuppagounder, S. S., Lee, S., Lee, J. H., Kim, W. R., Kook,
530 M., Foss, C. A., Shen, C., Lee, H., Kulkarni, S., Pasricha, P. J., Lee, G., Pomper, M. G., Dawson, V.
531 L., Dawson, T. M., & Ko, H. S. (2019). Transneuronal Propagation of Pathologic alpha-Synuclein
532 from the Gut to the Brain Models Parkinson's Disease. *Neuron*, *103*(4), 627-641 e627.
533 https://doi.org/10.1016/j.neuron.2019.05.035
534 Koga, S., Sekiya, H., Kondru, N., Ross, O. A., & Dickson, D. W. (2021). Neuropathology and molecular
535 diagnosis of Synucleinopathies. *Mol Neurodegener*, *16*(1), 83. https://doi.org/10.1186/s13024-
536 021-00501-z
537 Le, T. T., Trang, N. T., Pham, V. T. T., Quang, D. N., & Phuong Hoa, L. T. (2023). Bioactivities of beta-
538 mangostin and its new glycoside derivatives synthesized by enzymatic reactions. *R Soc Open Sci*,
539 *10*(8), 230676. https://doi.org/10.1098/rsos.230676
540 Lin, Y. C., Boone, M., Meuris, L., Lemmens, I., Van Roy, N., Soete, A., Reumers, J., Moisse, M., Plaisance,
541 S., Drmanac, R., Chen, J., Speleman, F., Lambrechts, D., Van de Peer, Y., Tavernier, J., &
542 Callewaert, N. (2014). Genome dynamics of the human embryonic kidney 293 lineage in
543 response to cell biology manipulations. *Nature Communications*, *5*.
544 https://doi.org/10.1038/ncomms5767
545 Lizazman, M. A., Jong, V. Y. M., Chua, P., Lim, W. K., & Karunakaran, T. (2022). Phytochemicals from
546 Calophyllum canum Hook f. ex T. Anderson and their neuroprotective effects. *Natural Product*
547 *Research*, 1-6.
548 Lopes, F. M., Bristot, I. J., da Motta, L. L., Parsons, R. B., & Klamt, F. (2017). Mimicking Parkinson's
549 Disease in a Dish: Merits and Pitfalls of the Most Commonly used Dopaminergic In Vitro Models.
550 *Neuromolecular Med*, *19*(2-3), 241-255. https://doi.org/10.1007/s12017-017-8454-x

Mathur, S., DeWitte, S., Robledo, I., Isaacs, T., & Stamford, J. (2015). Rising to the Challenges of Clinical Trial Improvement in Parkinson's Disease. *J Parkinsons Dis*, *5*(2), 263-268. https://doi.org/10.3233/JPD-150541

Mejía, M., Salgado-Bustamante, M., Castillo, C. G., & Jiménez-Capdeville, M. E. (2013). Passage determines toxicity and neuronal markers expression in PC12 cells with altered phenotype. *Toxicology Research*, *2*(6), 388-396. https://doi.org/10.1039/C3TX50010A

Ochu, E. E., Rothwell, N. J., & Waters, C. M. (1998). Caspases mediate 6-hydroxydopamine-induced apoptosis but not necrosis in PC12 cells. *J Neurochem*, *70*(6), 2637-2640. https://doi.org/10.1046/j.1471-4159.1998.70062637.x

Parekh, P., Sharma, N., Sharma, M., Gadepalli, A., Sayyed, A. A., Chatterjee, S., Kate, A., & Khairnar, A. (2022). AMPK-dependent autophagy activation and alpha-Synuclein clearance: a putative mechanism behind alpha-mangostin's neuroprotection in a rotenone-induced mouse model of Parkinson's disease. *Metabolic Brain Disease*, *37*(8), 2853-2870. https://doi.org/10.1007/s11011-022-01087-1

Parkhe, A., Parekh, P., Nalla, L. V., Sharma, N., Sharma, M., Gadepalli, A., Kate, A., & Khairnar, A. (2020). Protective effect of alpha mangostin on rotenone induced toxicity in rat model of Parkinson's disease. *Neurosci Lett*, *716*, 134652. https://doi.org/10.1016/j.neulet.2019.134652

Pokharel, S., Lee, C. H., Gilyazova, N., & Ibeanu, G. C. (2018). Analysis of Gene Expression and Neuronal Phenotype in Neuroscreen-1 (NS-1) Cells. *International journal of biomedical investigation*, *1*(3), 115. https://pubmed.ncbi.nlm.nih.gov/30687846

Ruan, J., Zheng, C., Liu, Y., Qu, L., Yu, H., Han, L., Zhang, Y., & Wang, T. (2017). Chemical and Biological Research on Herbal Medicines Rich in Xanthones. *Molecules*, *22*(10). https://doi.org/10.3390/molecules22101698

Ryou, M. G., & Mallet, R. T. (2018). An In Vitro Oxygen-Glucose Deprivation Model for Studying Ischemia-Reperfusion Injury of Neuronal Cells. *Methods Mol Biol*, *1717*, 229-235. https://doi.org/10.1007/978-1-4939-7526-6_18

Sasaki, A., Arawaka, S., Sato, H., & Kato, T. (2015). Sensitive western blotting for detection of endogenous Ser129-phosphorylated α-synuclein in intracellular and extracellular spaces. *Scientific reports*, *5*, 14211. https://doi.org/10.1038/srep14211

Sayyaed, A., Saraswat, N., Vyawahare, N., & Kulkarni, A. (2023). A detailed review of pathophysiology, epidemiology, cellular and molecular pathways involved in the development and prognosis of Parkinson's disease with insights into screening models. *Bulletin of the National Research Centre*, *47*(1). https://doi.org/10.1186/s42269-023-01047-4

Schober, A. (2004). Classic toxin-induced animal models of Parkinson's disease: 6-OHDA and MPTP. *Cell Tissue Res*, *318*(1), 215-224. https://doi.org/10.1007/s00441-004-0938-y

Shaw, G., Morse, S., Ararat, M., & Graham, F. L. (2002). Preferential transformation of human neuronal cells by human adenoviruses and the origin of HEK 293 cells. *Faseb j*, *16*(8), 869-871. https://doi.org/10.1096/fj.01-0995fje

Stoker, T. B., & Barker, R. A. (2020). Recent developments in the treatment of Parkinson's Disease. *F1000Res*, *9*. https://doi.org/10.12688/f1000research.25634.1

Tang, Y., Cui, Y., Luo, F., Liu, X., Wang, X., Wu, A., Zhao, J., Tian, Z., & Wu, L. (2012). Cell viability and dopamine secretion of 6-hydroxydopamine-treated PC12 cells co-cultured with bone marrow-derived mesenchymal stem cells. *Neural Regen Res*, *7*(14), 1101-1105. https://doi.org/10.3969/j.issn.1673-5374.2012.14.009

Ungerstedt, U. (1968). 6-Hydroxy-dopamine induced degeneration of central monoamine neurons. *Eur J Pharmacol*, *5*(1), 107-110. https://doi.org/10.1016/0014-2999(68)90164-7

Vareslija, D., Tipton, K. F., Davey, G. P., & McDonald, A. G. (2020). 6-Hydroxydopamine: a far from simple neurotoxin. *J Neural Transm (Vienna)*, *127*(2), 213-230. https://doi.org/10.1007/s00702-019-02133-6

Visanji, N. P., Kovacs, G. G., & Lang, A. E. (2021). The Discovery of α-Synuclein in Lewy Pathology of Parkinson's Disease: The Inspiration of a Revolution. *Mov Disord Clin Pract*, *8*(8), 1189-1193. https://doi.org/10.1002/mdc3.13312

Wagner, P. D., Vu, N. D., & Wu, Y. N. (1993). Pc12-Cells as a Model for Neuronal Secretion. *Botulinum and Tetanus Neurotoxins*, 105-115. <Go to ISI>://WOS:A1993BY71A00013

Wiesinger, J. A., Buwen, J. P., Cifelli, C. J., Unger, E. L., Jones, B. C., & Beard, J. L. (2007). Down-regulation of dopamine transporter by iron chelation in vitro is mediated by altered trafficking, not synthesis. *J Neurochem*, *100*(1), 167-179. https://doi.org/10.1111/j.1471-4159.2006.04175.x

Zhang, G., Buchler, I. P., DePasquale, M., Wormald, M., Liao, G., Wei, H., Barrow, J. C., & Carr, G. V. (2019). Development of a PC12 cell based assay for screening catechol-O-methyltransferase inhibitors. *ACS Chemical Neuroscience*, *10*(10), 4221-4226. https://www.ncbi.nlm.nih.gov/pmc/articles/PMC7032882/pdf/cn9b00395.pdf

628

manuscript KSJ

ORIGINALITY REPORT

8%	4%	8%	5%
SIMILARITY INDEX	INTERNET SOURCES	PUBLICATIONS	STUDENT PAPERS

PRIMARY SOURCES

1	Submitted to universititeknologimara Student Paper	3%
2	PinFen Chua, William K. Lim. "The strategic uses of collagen in adherent cell cultures", Cell Biology International, 2022 Publication	1%
3	ir.unimas.my Internet Source	1%
4	William K. Lim, Kimon C. Kanelakis, Richard R. Neubig. "Regulation of G protein signaling by the 70kDa heat shock protein", Cellular Signalling, 2013 Publication	1%
5	www.scielo.br Internet Source	1%
6	www.spandidos-publications.com Internet Source	1%

Exclude quotes	On	Exclude matches	< 1%
Exclude bibliography	On		